rate at each point studied. At 2.3 Bev/c a proton can create delta rays above the Čerenkov threshold in the gas counters and so cause a spurious coincidence, since its velocity is also high enough to be acceptable to the time-of-flight circuit. This background rate increases with increasing gas density in the counters, as can be seen from Fig. 1(b). Assuming that a counting rate corresponding to any particular mass value of three standard deviations above background would have been interpreted as significant, one arrives at an upper limit of about 3×10^{-6} for the proportion of particles of mass approximately 1400 m_e in the secondary beam.

PHYSICAL REVIEW VOLUME 123, NUMBER 2 JULY 15, 1961

Pion Production in Electron-Positron Collisions*

FRANK CHILTON†
Department of Physics, University of Chicago, Chicago, Illinois,
and
Department of Physics, University of Washington, Seattle, Washington

(Received March 13, 1961)

The properties due to the presence of symmetries in pion production processes in electron-positron collisions are discussed. Cross sections are calculated for the production reactions $e^+ + e^- \to \pi^0 + \gamma$, $e^+ + e^- \to e^+ + e^- + \pi^0$, and $e^+ + e^- \to \pi^+ + \pi^-$. The photon spectrum for the reaction $e^+ + e^- \to \pi^+ + \pi^- + \gamma$ is also calculated. The role of form factors and some of the possible effects of resonant strong interactions are discussed.

I. INTRODUCTION

THE prospect of clashing electron-positron beams is certainly an attractive one.[1,2] The electron-positron system possesses simplifying features because of its high degree of symmetry. In addition, many interesting particle production processes occur with cross sections proportional to the same order of the electromagnetic coupling constant as the cross section for $e^+ + e^-$ elastic scattering. Examples of such processes are the production of $\mu^+ + \mu^-$, $\pi^+ + \pi^-$, and $K^+ + K^-$ pairs. Further, such experiments offer an unambiguous way of studying certain strong interactions between pairs of particles in situations which are not complicated by the presence of additional strongly interacting particles.

Because of the presumably fundamental role of the pion in strong interactions, perhaps the most fundamental of these possible experiments are those involving pion production. Some of the symmetry properties relevant to these pion production processes are discussed in Sec. II. In Sec. III the results of calculations of π^0 production cross sections are given. Section IV contains the results of calculations for $\pi^+ + \pi^-$ pair production and the associated process of $\pi^+ + \pi^- + \gamma$ production, i.e., radiative pion pair production. Some discussion is given of the most likely effects of strong interactions, such as the introduction of form factors and the occurrence of resonances. Since the techniques of quantum electrodynamics are now well known,[3,4] calculational matters are only sketched, and this is done in the Appendix. The conventions used are those of Feynman.[3]

II. SYMMETRY CONSIDERATIONS

Since the electron and the positron form a particle-antiparticle pair, one has the possibility of charge conjugation invariance in addition to the usual symmetries such as space inversion, rotational invariance, and Lorentz invariance. It will be seen that this additional symmetry is of prime importance in most of the examples to be discussed, just as it is extremely useful in positronium.[4,5]

For high-energy scattering problems the conventional formalism, which involves an analysis into spin and orbital angular momentum states, is inconvenient. A

* Supported in part by the U. S. Atomic Energy Commission. The major portion of this work was done while the author was a National Science Foundation Predoctoral Fellow at the University of Chicago. A version of this work was submitted as a thesis to the faculty of the Department of Physics of the University of Chicago.

† Present address: Department of Physics, University of Washington, Seattle, Washington.

[1] Yung Su Tsai, Phys. Rev. **120**, 269 (1960). For experimental details related to proposed electron-electron scattering experiments, see W. C. Barber, B. Richter, W. K. H. Panofsky, G. K. O'Neill, and B. Gittelman, High-Energy Physics Laboratory Report, Stanford University HEPL-170 (unpublished). Additional information on the electron-electron experiment is given by W. K. H. Panofsky and Yung Su Tsai, *Proceedings of the 1960 Annual International Conference on High-Energy Physics at Rochester* (Interscience Publishers, Inc., New York, 1960), pp. 769, 771. For plans for electron-positron colliding beam experiments and details of the Frascati storage ring see B. Touschek *et al.*, Nuovo cimento **18**, 1293 (1960).

[2] N. Cabibbo and R. Gatto, Phys. Rev. Letters **4**, 313 (1960).

[3] R. P. Feynman, *The Theory of Fundamental Processes* (Cornell University, Ithaca, New York, unpublished).

[4] J. M. Jauch and F. Rohrlich, *The Theory of Photons and Electrons* (Addison-Wesley Publishing Company, Inc., Cambridge, 1955). For a discussion of positronium see Chap. 12, Sec. 5.

[5] L. Wolfenstein and D. G. Ravenhall, Phys. Rev. **88**, 279 (1952).

TABLE I. Eigenstates of **P** and **C** and their eigenvalues.

State	P	C
$t_+^{JM}=2^{-\frac{1}{2}}(\|JM;+-\rangle+\|JM;-+\rangle)$	$(-1)^J$	$(-1)^J$
$t_-^{JM}=2^{-\frac{1}{2}}(\|JM;+-\rangle-\|JM;-+\rangle)$	$(-1)^{J+1}$	$(-1)^{J+1}$
$t_0^{JM}=2^{-\frac{1}{2}}(\|JM;++\rangle+\|JM;--\rangle)$	$(-1)^J$	$(-1)^J$
$s^{JM}=2^{-\frac{1}{2}}(\|JM;++\rangle-\|JM;--\rangle)$	$(-1)^{J+1}$	$(-1)^J$

formalism based on states of total angular momentum and helicity, such as that of Jacob and Wick,[6] is especially suitable for relativistic particles. In this formalism the two-particle state in the barycentric frame is expressed as a direct product of one-particle states of opposite momenta and with their spins quantized only along their momenta, i.e., states of definite helicity. These plane-wave product states are then decomposed, using the familiar representation coefficients $\mathfrak{D}_{M\lambda}^{J}$,[7] into a sum of states $|JM;\lambda_1\lambda_2\rangle$ for which the total angular momentum is J, the z component of angular momentum is M, and the total helicity is $\lambda=\lambda_1-\lambda_2$. To describe a two-particle state in some other frame, it is only necessary to apply the appropriate rotation or Lorentz transformation operator. In constructing two-particle states for the electron-positron system in the usual Dirac formalism, one should remember that while the electron is represented by the Dirac spinor $\psi_{\lambda 1}(q_1)$, the positron is usually represented by an adjoint spinor $\bar{\psi}_{\lambda 2}(-q_2)$.

The behavior of the states $|JM;\lambda_1\lambda_2\rangle$ under the parity operator **P**, and the charge conjugation operator **C**, is given by

$$\mathbf{P}|JM;\lambda_1\lambda_2\rangle=(-1)^J|JM;-\lambda_1-\lambda_2\rangle, \quad (1)$$

and

$$\mathbf{C}|JM;\lambda_1\lambda_2\rangle=(-1)^J|JM;\lambda_2\lambda_1\rangle. \quad (2)$$

Relation (1) is given by Jacob and Wick.[6] Relation (2) can be derived by explicitly examining the result of **C** on a state (remembering to use $\bar{\psi}$ for the positron) or, more easily, by examining the triplet and singlet helicity states in Table I and recalling that in positronium $CP=+1$ for triplet states and $CP=-1$ for singlet states.

The combinations of $|JM;\lambda_1\lambda_2\rangle$ that are eigenstates of **P** and **C** are listed in Table I along with the corresponding eigenvalues for **P** and **C**. Note that the states t_+^{JM} and t_0^{JM} have the same eigenvalues. The same situation occurs in the analysis of positronium. Also note that the four states satisfy the usual conditions of orthonormality.

Table I can be used to decide which of the four states can possibly contribute to a reaction resulting in various particles in a state of total angular momentum J.

The process

$$e^+ + e^- \rightarrow \pi^0 + \gamma \quad (3)$$

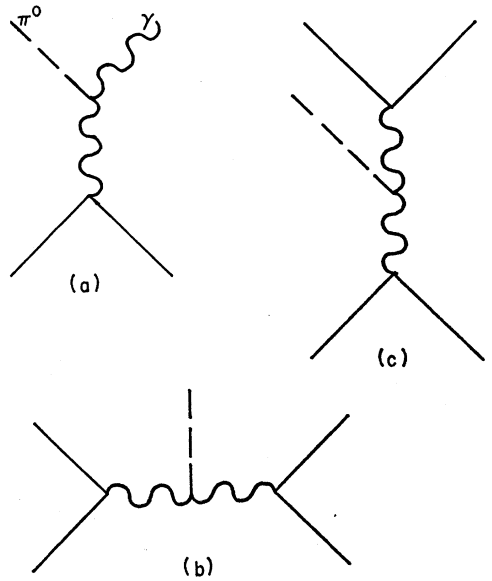

FIG. 1. Feynman diagrams for π^0 meson production: (a) $e^+ + e^- \rightarrow \pi^0 + \gamma$; (b) and (c) $e^+ + e^- \rightarrow e^+ + e^- + \pi^0$.

results in a π^0 mseon and involves only two particles in the final state. The $\pi^0+\gamma$ system has $C=-1$ regardless of the value of J. If J is odd and $P=-1$, then Table I indicates that the possible initial states are t_+^{JM} and t_0^{JM}; if $P=+1$, then only s^{JM} can contribute. Alternatively, if J is even, then only the state t_-^{JM} can contribute, which necessarily requires that $P=-1$. A Feynman diagram representing the lowest-order contribution to this process is shown in Fig. 1(a). The phenomenological interaction is discussed in Sec. III. Notice that interaction takes place through a single virtual photon. Consider a virtual photon associated with four-momentum, k. In the barycentric frame of the emitting or absorbing particle-antiparticle pair, $\mathbf{k}=0$. Thus the gauge condition, $k_0A_0-\mathbf{k}\cdot\mathbf{A}=0$, implies that $A_0=0$ and only a vector potential is possible. Thus the initial state is a vector, i.e., $J=1$, $P=-1$. Annihilation into a single virtual photon also requires $C=-1$. From Table I it is evident that t_+^{JM} and t_0^{JM} have the quantum numbers $P=-1$, $C=-1$ for $J=1$. However, it will be explicitly shown later in this section that the states t_0^{JM} do not, in fact, contribute to an electromagnetic interaction such as that of Fig. 1(a). Thus the initial state is necessarily t_+^{JM} with $J=1$.

Another π^0 meson production reaction is

$$e^+ + e^- \rightarrow e^+ + e^- + \pi^0. \quad (4)$$

The initial state is best analyzed in its barycentric frame, while the final state is best analyzed in the barycentric frame of the final $e^+ + e^-$ pair. The total eigenvalues of **P** and **C** are the same, of course. Since, for the π^0 meson, $C=+1$ holds, the value of C for the final state is simply the value of C for the final $e^+ + e^-$ pair, which depends on the total angular momentum j

[6] M. Jacob and G. C. Wick, Ann. Phys. 7, 404 (1959).
[7] E. P. Wigner, *Group Theory* (Academic Press, Inc., New York, 1959), Chap. 15.

of this pair. The value of P in the final state is the product of the parity of a π^0 meson with orbital angular momentum L, and the parity of the final $e^+ + e^-$ pair. Since parity and charge conjugation must be conserved in electromagnetic processes, the relation between the eigenvalues of the initial and final states can be written as

$$\langle J|\mathbf{C}|J\rangle = \langle j|\mathbf{C}|j\rangle, \tag{5a}$$

and

$$\langle J|\mathbf{P}|J\rangle = (-1)^{L+1}\langle j|\mathbf{P}|j\rangle. \tag{5b}$$

The four states of Table I are collectively represented as $|J\rangle$ and $|j\rangle$, for the initial and final states, respectively. Since each of these four states is an eigenstate of $\mathbf{P}$ and $\mathbf{C}$, the relations (5) just present the restrictions on the eigenvalues for the possible initial and final states. These restrictions constrain $J+j$ and L to be even or odd. The results are summarized in Table II. Only the upper half of the table need be written, since the relations (5) hold whether $|J\rangle$ is the initial state and $|j\rangle$ the final state or conversely. Even and odd are denoted by 0 and 1, respectively.

The diagrams representing the lowest-order contributions to the reaction (4) are shown in Fig. 1(b) and 1(c). An attempt to apply symmetry considerations to Fig. 1(b) gave no useful qualitative information. This diagram corresponds to the emission of virtual photons by both the electron and the positron, and many initial and final states are possible. The contribution of Fig. 1(b) will be discussed quantitatively in Sec. III. Explicit calculation showed that there was no interference between diagrams 1(b) and 1(c) in the pion spectrum or total cross section (after integration over electron and positron phase space). The diagram of Fig. 1(c) involves features discussed above. Since each $e^+ + e^-$ pair is connected to a single virtual photon, the argument given above applies to each pair in its barycentric frame. The electron-positron states corresponding to Fig. 1(c) are both vectors, i.e., $J=1$ and $j=1$. Again, the interaction is of a type that excludes the possibility of $t_0{}^{JM}$ contributing, as will be seen later. Inspection of Table II indicates, therefore, that the initial and final states must be the same (except possibly for the z component of angular momentum).

TABLE II. Even and odd restrictions on $J+j$ and resulting parity of L for the reaction $e^+ + e^- \to e^+ + e^- + \pi^0$.

Initial state	Final state $t_+{}^{jm}$	$t_-{}^{jm}$	$t_0{}^{jm}$	s^{jm}
$t_+{}^{JM}$	$J+j=0$ $L=1$	$J+j=1$ $L=1$	$J+j=0$ $L=1$	$J+j=0$ $L=0$
$t_-{}^{JM}$		$J+j=0$ $L=1$	$J+j=1$ $L=1$	$J+j=1$ $L=0$
$t_0{}^{JM}$			$J+j=0$ $L=1$	$J+j=0$ $L=0$
s^{JM}				$J+j=0$ $L=1$

Thus the possible transitions are $t_+{}^{JM} \to t_+{}^{jm}$, $t_-{}^{JM} \to t_-{}^{jm}$, and $s^{JM} \to s^{jm}$, with $J=j=1$.

Perhaps the most important capability of clashing electron-positron beams is the production of other particle-antiparticle pairs. These pairs will be produced electrodynamically without the presence of other strongly interacting particles which would make the analysis of interactions ambiguous. For instance, the process

$$e^+ + e^- \to \pi^+ + \pi^- \tag{6}$$

would produce a pair of pions without the presence of nucleons and would furnish a very clean way of studying the $\pi-\pi$ interaction. As a contrast, consider the difficulties which are present[8] in obtaining precise information on the $\pi-\pi$ interaction from the reaction $\pi^- + p \to \pi^+ + \pi^- + n$.

A $\pi^+ + \pi^-$ meson pair in a state of definite angular momentum J has $P=C=(-1)^J$, since the pion is spinless. Thus, only the initial states $t_+{}^{JM}$ and $t_0{}^{JM}$ can contribute. The lowest-order contribution to this

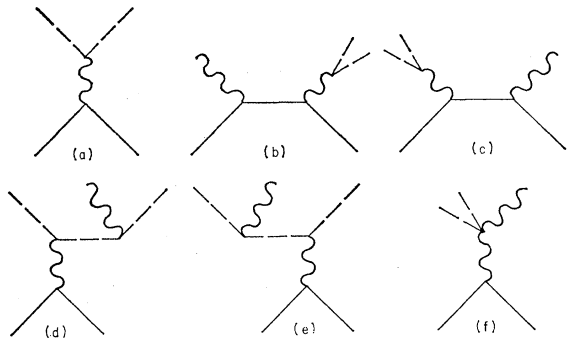

FIG. 2. Feynman diagrams for $\pi^+ + \pi^-$ pair production and radiative pair production: (a) pair production; (b)–(f) radiative pair production.

process is represented by the diagram, Fig. 2(a). Just as we have seen before, in the discussion of the amplitude for Fig. 1(a), the initial state must have $J=1$, $P=-1$, and $C=-1$. Thus the initial state must be $t_+{}^{JM}$ with $J=1$.

A $\pi^+ + \pi^-$ meson pair can also be produced with a photon,

$$e^+ + e^- \to \pi^+ + \pi^- + \gamma. \tag{7}$$

The analysis is best carried out for the initial state in its barycentric frame, and for the final state in the barycentric frame of the meson pair, in a fashion similar to the analysis of reaction (4). A pion pair with angular momentum j and an L-pole photon have $C=(-1)^{j+1}$, and $P=(-1)^{j+L}$ for electric multipoles, or $P=(-1)^{j+L+1}$ for magnetic multipoles. Using Table I, we obtain even and odd restrictions on $J+j$ and L for the various possible initial states of the total

[8] G. Chew and F. Low, Phys. Rev. **113**, 1640 (1959); S. D. Drell and F. Zachariasen, Phys. Rev. Letters **5**, 66 (1960).

angular momentum J. Table III lists these even and odd restrictions.

Figures 2(b)–(f) present the Feynman diagrams corresponding to the lowest-order contributions to radiative pion pair production, reaction (7). The meson pair in Figs. 2(b) and (c) is produced by a single virtual photon. This implies that $j=1$ for these diagrams. Since $C=-1$ for photons, the value of C for the process corresponding to Figs. 2(b) and 2(c) is $+1$. However, the final state corresponding to Figs 2(d)–(f) is produced by one virtual photon, indicating that $C=-1$ for these diagrams. However, since the photon in the final state has $C=-1$, this is only possible if these three diagrams correspond to even values of j. Since the meson states for different j are orthogonal, the integration over pion phase space will eliminate any interference between the terms corresponding to Figs. 2(b) and (c) and the terms corresponding to Figs. 2(d)–(f).

It is worthwhile at this point to consider the symmetry properties of some other possible final states involving mesons, even though no quantitative considerations are to be given in this paper. Since pions satisfy Bose-Einstein statistics, a system consisting of two π^0 mesons must necessarily have even angular momentum in their barycentric frame; such a system would have $C=+1$ and $P=+1$. From Table I it is clear that only the initial states $t_+{}^{JM}$ and $t_0{}^{JM}$ can possibly contribute to the production of two π^0 mesons, and only for even J. Note that a single virtual photon could not be an intermediate state resulting in the production of two π^0 mesons. The detailed mechanism of π^0 pair production need not be the same as the phenomenological interaction between the π^0 meson and the electromagnetic field. For instance, one can imagine a process in which a $\pi^+ + \pi^-$ pair is produced and interacts strongly to produce a pair of π^0 mesons. In terms of isospin, this would indicate that the $I=0$ and $I=2$ amplitudes were not equal.

The three-pion system $\pi^+ + \pi^- + \pi^0$ also has simple symmetry properties. If the $\pi^+ + \pi^-$ meson pair have a relative angular momentum j_1, and the π^0 meson has angular momentum j_2, relative to the center of momentum of the $\pi^+ + \pi^-$ pair, then the system has $P=(-1)^{j_1+j_2+1}$, $C=(-1)^{j_1}$ and $CP=(-1)^{j_2+1}$. However, these are not quite enough quantum numbers to uniquely determine the state of the $\pi^+ + \pi^- + \pi^0$ system. A possible complete set of observables for this system would be the total angular momentum J, the z component of angular momentum, C, P, the total energy and momentum of the system, and a quantity specifying the relative distribution of energy between the π^0 meson and the $\pi^+ + \pi^-$ pair.

A muon pair $\mu^+ + \mu^-$ would have the same symmetry properties as the incoming electron-positron state. The lowest-order process would proceed through one virtual photon and the muon and electron-positron states involved would be $t_+{}^{JM}$ with $J=1$.

TABLE III. Even and odd restrictions on $J+j$ and the resulting parity of L for the reaction $e^+ + e^- \to \pi^+ + \pi^- + \gamma$.

State	$J+j$	L-electric	L-magnetic
$t_+{}^{JM}$	1	1	0
$t_-{}^{JM}$	0	1	0
$t_0{}^{JM}$	1	1	0
s^{JM}	1	0	1

In practice, one is not so much interested in the properties of initial states of definite J as those of plane-wave states. In a fashion analogous to the definition of the eigenstates of **P** and **C**, one can define helicity-correlated plane-wave states for electron-positron pairs. These states are combinations of two-particle plane-wave states of definite helicity $|\mathbf{q};\lambda_1\lambda_2\rangle$, where the electron has momentum $\mathbf{q}$ and helicity λ_1, while the positron has momentum $-\mathbf{q}$ and helicity λ_2. The four states are

$$\begin{aligned} t_+(\mathbf{q}) &= 2^{-\frac{1}{2}}(|\mathbf{q};+-\rangle + |\mathbf{q};-+\rangle), \\ t_-(\mathbf{q}) &= 2^{-\frac{1}{2}}(|\mathbf{q};+-\rangle - |\mathbf{q};-+\rangle), \\ t_0(\mathbf{q}) &= 2^{-\frac{1}{2}}(|\mathbf{q};++\rangle + |\mathbf{q};--\rangle), \\ s(\mathbf{q}) &= 2^{-\frac{1}{2}}(|\mathbf{q};++\rangle - |\mathbf{q};--\rangle). \end{aligned} \tag{8}$$

Using relations provided by Jacob and Wick[6] one can expand these states (8), as a sum of the states of definite J, M given in Table I. Since the states $t_0(\mathbf{q})$ and $s(\mathbf{q})$ have zero total helicity, $\lambda=0$, they may be expressed as sums over the states $t_0{}^{JM}$ and the states s^{JM}, respectively. On the other hand, $t_+(\mathbf{q})$ and $t_-(\mathbf{q})$ have parts of total helicity $\lambda=\pm 1$, and are each equal to a sum including both $t_+{}^{JM}$ and $t_-{}^{JM}$ states with total helicities ± 1. This is quite understandable from another point of view. The plane-wave state corresponds to an electron of momentum $\mathbf{q}$ and helicity λ_1, and positron with $-\mathbf{q}, \lambda_2$. But the charge conjugate state would have an electron with $-\mathbf{q}, \lambda_2$, and a positron with $\mathbf{q}, \lambda_1$. If $\lambda_1=\lambda_2$, then the charge conjugate state is the same as a state which has had only the space-dependent parts reversed. However, if $\lambda_1=-\lambda_2$, then the charge conjugate state is the same as a state which has had both its space dependence and helicity reversed.

The expectation value of the helicity operator vanishes for all the states (8). The states $t_+(\mathbf{q})$ and $t_-(\mathbf{q})$ correspond to "linearly polarized" combinations of $|\mathbf{q};+-\rangle$ and $|\mathbf{q};-+\rangle$, which have helicities $+1$ and -1, respectively, and could appropriately be denoted $t_{+1}(\mathbf{q})$ and $t_{-1}(\mathbf{q})$, respectively.

To study the details of the electron-positron system in interaction, such as behavior in the relativistic limit, or in order to determine which of the states (8) can contribute through a given mechanism for interaction, it is sufficient to proceed in a pedestrian fashion and construct the explicit solutions to the Dirac equation. Since states of definite helicity are desired, the rela-

tivistic representation[9] of the γ matrices is used,

$$\gamma_0=\begin{pmatrix}0 & I\\ I & 0\end{pmatrix},\qquad \boldsymbol{\gamma}=\begin{pmatrix}0 & -\boldsymbol{\sigma}\\ \boldsymbol{\sigma} & 0\end{pmatrix},$$
$$i\gamma_5=\begin{pmatrix}-I & 0\\ 0 & I\end{pmatrix},\quad \gamma\cdot q=\gamma_0 Q-\boldsymbol{\gamma}\cdot\mathbf{q}. \tag{9}$$

Taking $\mathbf{q}$ along the z axis, the solutions for the electron are

$$\psi(q_1)=[2(Q+m)]^{-\frac{1}{2}}\begin{pmatrix}Q+q\sigma_3+m\\ Q-q\sigma_3+m\end{pmatrix}u_{\lambda 1}, \tag{10}$$

where $\bar{\psi}\psi=2m$, while those for the positron are

$$\bar{\psi}(-q_2)=[2(Q+m)]^{-\frac{1}{2}}u_{\lambda 2}{}^{\dagger}(Q+q\sigma_3+m,\ -(Q-q\sigma_3+m)), \tag{11}$$

where $\bar{\psi}\psi=-2m$, $q_1=(Q,\mathbf{q})$, $q_2=(Q,-\mathbf{q})$, and $u_{\lambda 1}$, $u_{\lambda 2}$ are Pauli spinors whose components correspond to helicity $\pm\frac{1}{2}$. Any amplitude involving the electron-positron system will always contain both $\psi(q_1)$ and $\bar{\psi}(-q_2)$ together. But since $\sum_{rs}\bar{\psi}_r A_{rs}\psi_s=\mathrm{Tr}[\psi\bar{\psi}A]$ for any matrix A, one can consider the electron-positron system to be represented by the 4×4 state matrix, $\psi(q_1)\bar{\psi}(-q_2)$, in spin space. To form any bilinear combination one simply takes the trace (paying careful attention to order). Actually, a 4×4 matrix is not necessary; attention could be confined only to a 2×2 matrix, since the electron and positron each have only two spin states. In fact, it is easy to verify that for the states (8) $u_{\lambda 1}u_{\lambda 2}{}^{\dagger}$ forms a matrix which is just one of the Pauli matrices or the unit matrix. However, the Dirac theory is most familiar in its four-component form, instead of its two-component form, and shall be treated in that fashion here.

Selecting electron states from (10) and positron states from (11), forming the Kronecker products $\psi(q_1)\bar{\psi}(-q_2)$, and combining in the manner required by (8) gives a 4×4 matrix for each of the four states (8). These 4×4 matrices can then be expressed in terms of the γ matrices to give

$$\begin{aligned}
t_+(\mathbf{q})&=2^{-\frac{1}{2}}(Q\gamma_1+qi\gamma_2 i\gamma_5+m\gamma_0\gamma_1),\\
t_-(\mathbf{q})&=2^{-\frac{1}{2}}(Qi\gamma_2+q\gamma_1 i\gamma_5+m\gamma_0 i\gamma_2),\\
t_0(\mathbf{q})&=-2^{-\frac{1}{2}}(Qi\gamma_5+q\gamma_0\gamma_3 i\gamma_5+m\gamma_0 i\gamma_5),\\
s(\mathbf{q})&=2^{-\frac{1}{2}}(Q\gamma_0\gamma_3+qI+m\gamma_3).
\end{aligned} \tag{12}$$

Note that the last term is always $mQ^{-1}\gamma_0$ times the first term. The three terms in each state matrix have different numbers of γ matrices (note that $\gamma_5=\gamma_1\gamma_2\gamma_3\gamma_0$ is a product of four γ matrices); therefore each will contribute to a given amplitude in a different way. Behavior in the relativistic limit is quite clear; the last term is of order m/Q compared to the first two terms, and can be neglected. In the relativistic limit $t_+(\mathbf{q})$ and $t_-(\mathbf{q})$ have an odd number of γ matrices while $t_0(\mathbf{q})$ and $s(\mathbf{q})$ have an even number of γ matrices.

[9] D. R. Yennie, D. G. Ravenhall, and R. N. Wilson, Phys. Rev. **95**, 500 (1954); J. Hamilton, *The Theory of Elementary Particles* (Oxford University Press, New York, 1959), Chap. 3, Sec. 10.

TABLE IV. Explicit forms for the bilinear covariants.[a]

State	$\bar{\psi}\psi$	$\bar{\psi}i\gamma_5\psi$	$\bar{\psi}\gamma^\mu\psi A_\mu$	$\bar{\psi}i\gamma_5\gamma^\mu\psi B_\mu$	$\frac{1}{2}\bar{\psi}\sigma^{\mu\nu}\psi T_{\mu\nu}$[b]
$t_+(\mathbf{q})$	0	0	$-QA_1$	qiB_2	mT_{01}
$t_-(\mathbf{q})$	0	0	$-QiA_2$	qB_1	miT_{02}
$t_0(\mathbf{q})$	0	$-Q$	0	mB_0	qiT_{12}
$s(\mathbf{q})$	q	0	$-mA_3$	0	QT_{03}

[a] Each entry in the table should be multiplied by $4/\sqrt{2}$.
[b] $T_{\mu\nu}=-T_{\nu\mu}$.

The bilinear covariants for the electron-positron system in their barycentric frame are easily constructed; it is only necessary to take the appropriate trace. Table IV is a list of the bilinear covariants. Note that the state $t_0(\mathbf{q})$ cannot contribute to the current $\bar{\psi}(-q_2)\gamma^\mu\psi(q_1)$. Since the state $t_0(\mathbf{q})$ is equal to a sum over the states $t_0{}^{JM}$, this implies that initial states $t_0{}^{JM}$ cannot contribute to interactions such as those shown in Figs. 1(a), 2(a), 2(d) or 2(e). The relativistic limit for Table IV is evident. All terms multiplied by m are of order m/Q compared to the others and can be ignored.

The state matrices (12) and Table IV can be used to analyze the electron-positron part of a Feynman diagram. In the relativistic limit, only the matrices for $t_+(\mathbf{q})$ and $t_-(\mathbf{q})$ have an odd number of γ matrices. Thus, only these two states can contribute to diagrams such as Figs. 1(a), 2(a), 2(d) or 2(e), which have amplitudes proportional to $\bar{\psi}\gamma^\mu\psi$, or other annihilation type diagrams such as Figs. 2(b) and (c), which have amplitudes containing an odd number of γ matrices in the relativistic limit. This conclusion is obtainable from another point of view. In the relativistic limit, $\frac{1}{2}(1\mp i\gamma_5)\psi(q_1)$ represents an electron with helicity $\pm\frac{1}{2}$, while $\bar{\psi}(-q_2)\frac{1}{2}(1\mp i\gamma_5)$ represents a positron with helicity $\pm\frac{1}{2}$ (chirality anticommutes with charge conjugation).[10] Commuting the matrix $i\gamma_5$ through the amplitude, it is clear that, in the relativistic limit, only states of opposite helicity can contribute to an annihilation type of diagram.

III. π^0 MESON PRODUCTION

The process of lowest order in the electromagnetic coupling constant that results in π^0 meson production is the reaction (3). The Feynman diagram describing this process is shown in Fig. 1(a). The differential cross section was calculated using a phenomenological vertex for the coupling of a neutral pseudoscalar particle to two photons.[11] The matrix element for this coupling was taken as

$$\mathfrak{M}=(2g/\mu)\epsilon^{\alpha\beta\mu\nu}k_\alpha\mathcal{E}_\beta k_\mu'\mathcal{E}_\nu', \tag{13}$$

[10] J. J. Sakurai, *Invariance Principles and Elementary Particles* [Princeton University Press, Princeton, New Jersey (to be published)], Chap. 2.
[11] R. H. Dalitz, Proc. Phys. Soc. (London) **A64**, 667 (1951).

where g is a phenomenological coupling constant, μ is the mass of the π^0 meson, $\epsilon^{\alpha\beta\mu\nu}$ is the totally antisymmetric four-tensor density, and $\mathcal{E}_\beta$ and $\mathcal{E}_\nu'$ represent the photon polarizations, while k_α and k_μ' represent their respective four-momenta. After a calculation is completed, the coupling constant g is eliminated in favor of the lifetime τ, which is given by the relation

$$1/\tau = g^2\mu/16\pi. \tag{14}$$

The expression for the differential cross section in the barycentric frame of the $e^+ + e^-$ pair, for the reaction (3), in lowest order is $[\hbar = c = 1, \alpha = (137)^{-1}]$

$$(d\sigma/d\Omega) = (\alpha/2\pi\tau\mu^3)[1-(\mu/2Q)^2]^{\frac{1}{2}}(1+\cos^2\theta), \tag{15}$$

where Q is the electron (or positron) energy. The limit $m^2 = 0$ (vanishing electron mass) is taken, an excellent approximation at such high energies. The total cross section is

$$\sigma = (8\alpha/3\tau\mu^3)[1-(\mu/2Q)^2]^{\frac{3}{2}}. \tag{16}$$

Note that this cross section has an asymptotic upper bound in the high-energy limit. Numerical values of this cross section (16), are shown in Fig. 3(a). Since the lifetime of the π^0 meson is not yet known precisely,[12] the convenient value $\tau = 10^{-16}$ sec was used. The principal region of interest for π^0 meson production processes would presumably be for $0.5\mu \leq Q \leq 1\mu$, i.e., below the threshold for production of π^0 pairs.

The reaction (4) is the π^0 production process which results in a cross section of next-lowest order in the electromagnetic coupling constant. It will be seen shortly that the cross section is actually substantially larger than (16). Figures 1(b) and 1(c) are Feynman diagrams showing the lowest-order contributions to reaction (4). Some of the details which occurred in the calculation are discussed in the Appendix. For the barycentric frame of the electron-positron pair, the contributions to the spectral-differential cross section of the mesons produced are presented separately for diagrams 1(b), 1(c) and their interference in Eq. (17a), (17b), and (17c), respectively,

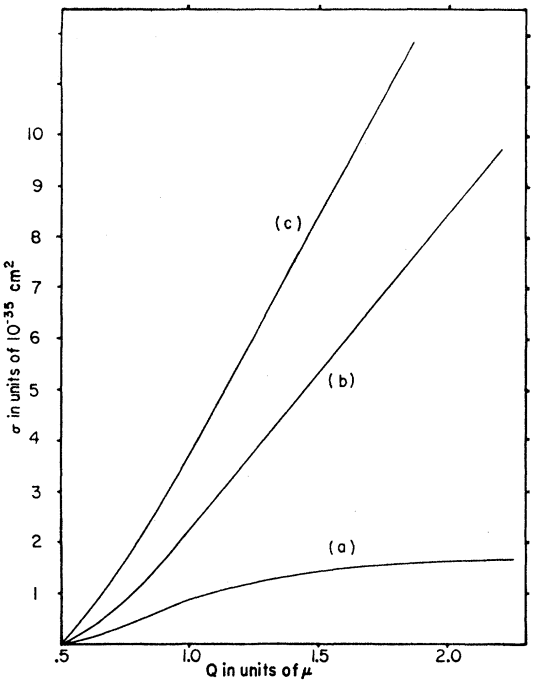

FIG. 3. Cross sections for π^0 meson production: (a) $e^+ + e^- \to \pi^0 + \gamma$; (b) $e^+ + e^- \to e^+ + e^- + \pi^0$ including all logarithmic terms; (c) $e^+ + e^- \to e^+ + e^- + \pi^0$ including only terms in $[\ln(2Q/m)]^2$.

$$\left.\frac{d^2\sigma}{dPd\Omega}\right|_{1(b)} = \frac{2}{\pi}\frac{\alpha^2}{\tau\mu^3}\frac{P^2}{Q^2E}\left\{\ln\frac{2Q}{m}\left[\frac{B}{4Q^2P^2A}+\frac{P^2A}{2G^2}+\frac{P^2A}{2H^2}+\frac{2P\xi}{G}-\frac{2P\xi}{H}\right]+\frac{2R^2}{P^2A}+\frac{B}{16Q^2P^2A}\ln\frac{R^4P^4A^2}{(R^4+4Q^2G^2)(R^4+4Q^2H^2)}\right.$$
$$\left.+\ln\frac{R^2G^2}{R^4+4Q^2G^2}\left[\frac{P^2A}{4G^2}+\frac{P\xi}{G}\right]+\ln\frac{R^2H^2}{R^4+4Q^2H^2}\left[\frac{P^2A}{4H^2}-\frac{P\xi}{H}\right]+\frac{1}{2}\frac{(R^2+P^2\xi^2)^2-P^4}{G^2H^2}-\frac{1}{2}\right\}, \tag{17a}$$

$$\left.\frac{d^2\sigma}{dPd\Omega}\right|_{1(c)} = \frac{8}{3\pi}\frac{\alpha^2}{\tau\mu^3}\frac{P^4}{Q^2R^2E}(1+\xi^2), \tag{17b}$$

and

$$\left.\frac{d^2\sigma}{dPd\Omega}\right|_{1(bc)} = \frac{2}{\pi}\frac{\alpha^2}{\tau\mu^3}\frac{P^3\xi}{Q^2R^2E}\left\{(4Q^2-R^2)\ln\frac{P^2A}{GH}+2\left[2Q^2-\frac{R^4}{GH}+\frac{Q(2Q-E)R^4}{G^2H^2}\right]\right\}, \tag{17c}$$

where $\xi = \cos\theta$, $A = 1-\beta^2\xi^2$, $R^2 = (2Q-E)^2-P^2$, $G = 2Q-E+P\xi$, $H = 2Q-E-P\xi$, and $B = (R^2+4Q^2)^2 + 16Q^2P^2\xi^2$. In Eq. (17), $\beta = q/Q$ is the electron momentum-to-energy ratio. The pion momentum and energy are P and E, respectively. Of course, the limit $m^2 = 0$ is taken, except where it would result in a singularity in the cross sections. Then a first-order term

[12] R. F. Blackie, A. Engler, and J. H. Mulvey, Phys. Rev. Letters **5**, 384 (1960); H. Ruderman, S. Berman, R. Gomez, A. V. Tollestrup, and R. Talman, Bull. Am. Phys. Soc. **5**, 508 (1960). A. V. Tollestrup, *et al.* and R. G. Glasser, *et al.*, *Proceedings of the 1960 Annual International Conference on High-Energy Physics at Rochester* (Interscience Publishers, Inc., New York, 1960), pp. 27, 30. For attempts to set limits on the lifetime see G. Harris, J. Orear, and S. Taylor, Phys. Rev. **106**, 327 (1957); M. Jacob and J. Mathews, *ibid.* **117**, 855 (1960).

in m^2 is also kept. The total spectral-differential cross section is the sum of (17a), (17b), and (17c).

The interference contribution Eq. (17c) is odd in $\cos\theta$ (θ is the production angle with respect to the forward direction); thus there will be no interference in the meson spectrum or total cross section.

Not all of the integrals over the meson angles in Eq. (17) can be performed in terms of tabulated functions. However, as discussed in the Appendix, a good approximation can be obtained by separating those terms which contribute as $[\ln(2Q/m)]^2$ and $\ln(2Q/m)$ to the total cross section.

Integration over pion angles, for the logarithmic terms only, yields the pion spectrum, normalized as a cross section,

$$\frac{d\sigma}{dP}=\frac{8\alpha^2}{\tau\mu^3}\frac{P^2}{Q^2E}\left\{\left(\ln\frac{2Q}{m}\right)^2\frac{B_1}{8Q^2P^2}+\ln\frac{2Q}{m}\left[\frac{2R^2}{P^2}-2-\frac{2Q-E}{P}\ln\frac{G_1}{H_1}+\frac{B_1}{16Q^2P^2}\left(4\ln 2+\ln\frac{P^4}{B_1}\right)\right]+\frac{8}{9}\frac{P}{H_1}\right\}. \quad (18)$$

The subscript 1 indicates that the quantity is to have its value when $\xi=1$. The last term in Eq. (18) is the only contribution corresponding to Fig. 1(c).

Not all of the logarithmic terms in the spectrum are integrable over the momentum in terms of tabulated functions. However, it is possible to extract the terms proportional to $[\ln(2Q/m)]^2$ in the total cross section. This leading term of the cross section is

$$\sigma=\frac{16\alpha^2}{\tau\mu^3}\frac{\{\ln[(\mu/m)\eta]\}^2}{\eta^4}[(2\eta^2+1)^2\ln\eta-(\eta^2-1)(3\eta^2+1)], \quad (19)$$

where $\eta=2Q/\mu$. The integration is from $P=0$ to $P_{\max}=Q-\mu^2/(4Q)$. This leading term of the cross section was correctly given by Low,[13] using an approach similar to the Weizsäcker-Williams method.[14,15]

Figure 4(a) presents some graphs of the pion momentum spectrum normalized as a cross section, for different values of the electron energy, ($\tau=10^{-16}$ sec). The curves are extended to the origin. For comparison, the curves for the $[\ln(2Q/m)]^2$ terms are presented separately, in Fig. 4(b). Notice that the $[\ln(2Q/m)]^2$ terms are almost canceled by the $\ln(2Q/m)$ terms near $P=0$. As expected, the Weizsäcker-Williams approach applies more accurately for higher energies. Numerical integration of (18) gives the total cross section, which is shown in Fig. 3(b). For comparison, the leading term of the total cross section (19) is shown in Fig. 3(c). Note that these cross sections are appreciably larger than Fig. 3(a) which corresponds to reaction (3). This is primarily due to the presence of the forward scattering pole in the contribution of Fig. 1(b) to the cross section. The contribution for this pole alone, which corresponds to real photons, is given by the Weizsäcker-Williams approach. It is interesting to note that the total cross sections seem to be nearly linear even at moderate energies above threshold.

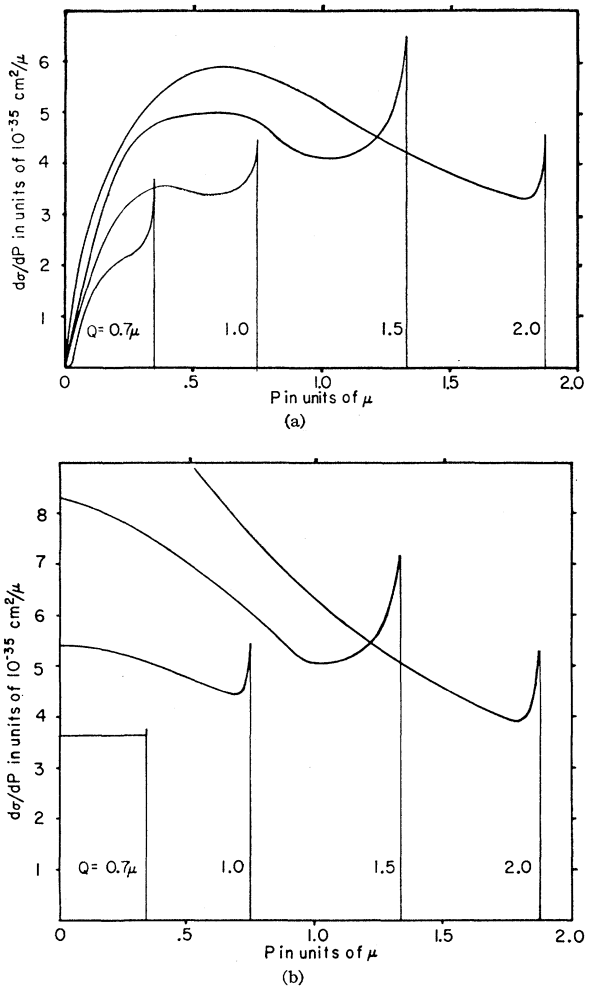

FIG. 4. Pion spectrum for $e^+ + e^- \rightarrow e^+ + e^- + \pi^0$: (a) including all logarithmic terms; (b) including only the leading term.

Since the contributions corresponding to Fig. 1(b) dominate the cross section, expressions (17a), (18), and (19) are fairly good approximations for π^0 meson production in electron-electron collisions. In fact, when the contributions due to Fig. 1(c) and its interference are omitted, expressions (17a), (18), and (19) correspond to a calculation ignoring exchange effects. The

[13] F. E. Low, Phys. Rev. **120**, 582 (1960).

[14] K. F. Weizsäcker, Z. Physik **88**, 612 (1934); E. J. Williams, Phys. Rev. **45**, 729 (1934); Kgl. Danske Videnskab. Selskab, Mat.-fys. Medd. **13**, 4 (1935); W. Heitler, *The Quantum Theory of Radiation* (Oxford University Press, New York, 1954), Appendix 6.

[15] R. H. Dalitz and D. R. Yennie, Phys. Rev. **105**, 1598 (1957); R. B. Curtis, *ibid.* **104**, 211 (1956).

numerical results of Figs. 3 and 4 are also fairly accurate, since the contributions corresponding to Fig. 1(c) did not become important until near $P=P_{\max}$, where they were only a percentage of the total spectrum.

Some work has been done on what possible effects strong interactions,[16] particularly various conjectured resonances, might have on the interaction of the π^0 meson with the electromagnetic field. Quite generally, such interactions would necessitate the introduction of a form factor $F(k_1^2,k_2^2)$, in the interaction (13), where k_1 and k_2 refer to the two photon lines. This form factor would, of course, be a symmetric function of k_1, k_2 since the photons are identical bosons. The neutral pion decay would correspond to $F(0,0)=1$.

The study of reaction (3) corresponding to Fig. 1(a) would provide, in principle, a way of directly measuring the form factor for large timelike momentum transfers since the cross section (16) would then be multiplied by $|F(4Q^2,0)|^2$. Although Fig. 3 shows that the cross section for reaction (3) is less than one-half of the cross section for reaction (4) for the energy region of interest, $0.5\mu\leq Q\leq 1\mu$, reaction (3) is a two-body reaction. Experimentally, the subsequent decay of the π^0 meson would give the unique signature of three high-energy γ rays of possibly wide angle and known energy relationships.

The role of the form factor in the cross section for reaction (4) is more complicated since the momentum transfers are not uniquely determined by kinematics in this case. As Low has pointed out,[13] the leading term of the cross section Eq. (19), corresponds to $F(0,0)=1$. The evaluations of other terms would require the inclusion of the form factor in the integrations.

IV. $\pi^+ + \pi^-$ PAIR PRODUCTION

Pion pair production is an example of a process which takes place in the same order of the electromagnetic coupling constant as elastic electron-positron scattering. The Feynman diagram for process (6) is shown in Fig. 2(a). The differential cross section is easily calculated.[1,2,17]

$$d\sigma/d\Omega=(\alpha^2/32)|F(4Q^2)|^2[(Q^2-\mu^2)^{\frac{3}{2}}/Q^5]\sin^2\theta. \quad (20)$$

While the presence of the form factor makes Eq. (20) quite general, it is included here, primarily in order to include the effect of possible interactions between the two pions. Integration of (20) over angles gives the total cross section,

$$\sigma=(\pi\alpha^2/12)|F(4Q^2)|^2[(Q^2-\mu^2)^{\frac{3}{2}}/Q^5]. \quad (21)$$

Figure 5(a) gives the value of the cross section, Eq. (21), assuming that only lowest-order quantum electrodynamics is necessary, i.e., $F(4Q^2)=1$. Figure 5(b) gives values for the same cross section if there is a $\pi-\pi$ resonance. Note the change of scale in the latter. The resonant form factor used was that of Frazer and Fulco,[18] which corresponds to a resonant energy $Q_{\text{res}}\approx 1.6\mu$ and a half-width approximately equal to μ. Of course, the parameters used here for the resonant cross section are intended primarily for illustration. The effect of the resonance is accentuated by the accidental circumstance that the peak of the Frazer-Fulco $\pi-\pi$ resonance has the same value for the momentum transfer as the maximum of the cross section obtained by a lowest-order quantum electrodynamics calculation.

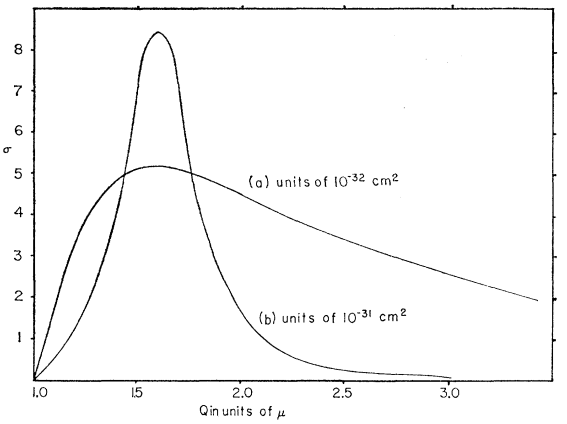

FIG. 5. Cross sections for $\pi^+ + \pi^-$ pair production: (a) from lowest order quantum electrodynamics only; (b) including a $\pi-\pi$ resonance.

Should a $\pi-\pi$ resonance exist, it will distort the photon energy spectrum for the radiative pion pair production process (7). For reactions (6) and (7) the momentum transfer to the pion pair is $4Q^2$ and $4Q(Q-\omega)$, respectively; ω is the photon energy. Therefore, in reaction (7) the position of the resonance is a function of both Q and ω.

The Feynman diagrams for the various contributions to radiative pair production are shown in Figs. 2(b)–(f). In Sec. II it was shown that the contributions from diagrams 2(b) and (c) do not interfere in the photon spectral differential cross section with the contributions from diagrams 2(d)–(f). Also the pions in the process of diagrams 2(b) and (c) are in a $J=1$ state, the particular state for which Frazer and Fulco conjectured a resonant interaction, while the pions for diagrams 2(d)–(f) are only in states of even angular momentum for which no one has (yet) had reason to conjecture any particular strong interaction.

The values of the photon spectrum normalized as a cross section for the two sets of diagrams are given separately,

$$\frac{d\sigma}{d\omega}=\frac{\alpha^3}{3Q^2}|F(R^2)|^2\left[\ln\frac{2Q}{m}\left(\frac{R^2}{\omega^2}+2\right)-1\right]\frac{S^3\omega}{R^5} \quad (22a)$$

[16] S. M. Berman and D. A. Geffen, Nuovo cimento **18**, 1192 (1960); How-sen Wong, Phys. Rev. **121**, 289 (1960).

[17] A. I. Nikishov, Soviet Phys.—JETP **36**, 937 (1959) (translation).

[18] W. Frazer and J. Fulco, Phys. Rev. **117**, 1609 (1960). Also see M. Baker and F. Zachariasen, *ibid.* **118**, 1659 (1960).

for Figs. 2(b) and (c) and

$$\frac{d\sigma}{d\omega}=\frac{\alpha^3}{48Q^4}\left\{\ln\frac{R+S}{R-S}\left[\frac{8Q^2R^2-13\mu^2R^2-12\mu^2Q^2+20\mu^4}{\omega R^2}+\frac{6(R^2-2QR-2\mu^2)+8Q^2}{R}+\frac{16Q^2\mu^2(R+Q)}{R^4}+\frac{4\mu^2\omega}{R^2}\right.\right.$$
$$\left.\left.+\frac{8Q\omega^2}{R^2}+\frac{16Q\omega^3}{R^3}\right]-\frac{2S}{R}\left[\frac{2Q^2-5\mu^2}{\omega}+\frac{3R^2-8QR-8Q^2}{R}+\frac{\omega(12Q^2+4QR-5R^2)}{R^2}+\frac{16Q^2\omega^2}{R^3}\right]\right\} \quad (22b)$$

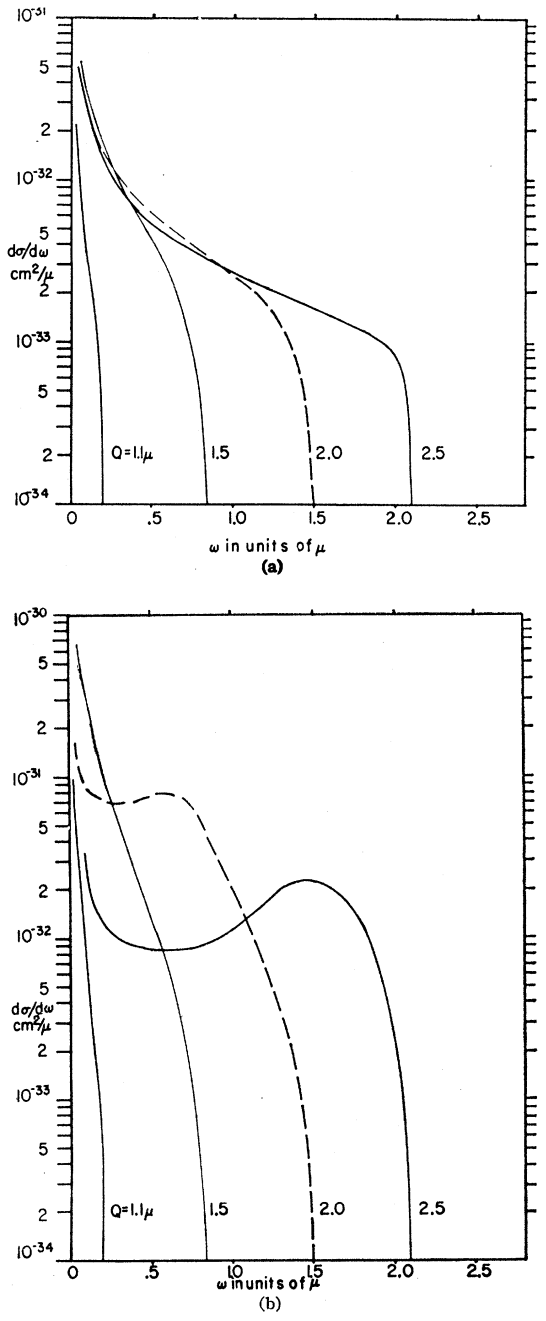

FIG. 6. Photon spectrum in radiative pion pair production: (a) from lowest-order quantum electrodynamics only; (b) including a $\pi-\pi$ resonance.

for Figs. 2(d)–(f). In these expressions,

$$R=[4Q(Q-\omega)]^{\frac{1}{2}},\quad S=[4Q(Q-\omega)-4\mu^2]^{\frac{1}{2}},$$

and ω is the photon energy with $\omega_{\max}=Q-\mu^2/Q$. The total spectrum is just the sum of (22a) and (22b). Intuitively, one might expect that the contribution from (22a), which corresponds to radiation from electron lines, would be larger than the contribution from (22b), which corresponds to radiation from pion lines by approximately a factor of $\ln(\mu/m)\approx 6$. This is more or less the case. It was found that near $\omega=0$, the ratio went from about 15 to 6 as Q increased from 1.1 μ to 2.5 μ, while for ω near $\omega_{\max}$ the ratio went from 4 to $\frac{1}{3}$ for the same values of Q. Figure 6(a) presents the spectrum given by Eqs. (22a) and (22b) with $F(R^2)=1$ for four values of Q. Note that as soon as the energy is substantially above the threshold, the shape of the dominate part of the spectrum (low ω) does not change appreciably with increasing Q. This is due to the dominance of the infrared divergent terms which do not change appreciably with Q. Most of the other terms remained constant or insignificant until past $\frac{1}{2}\omega_{\max}$. Figure 6(b) shows what could possibly happen to the spectrum if a $\pi-\pi$ resonance in the $J=1$ state does exist. The Frazer-Fulco form factor was used in expression (22a) in the calculation of the spectra in Fig. 6(b).

The distortions in the photon spectrum, should a $\pi-\pi$ resonance exist [Fig. 6(b)], could appreciably increase the inelastic radiative corrections to pion pair production for some experimental situations. As an example, consider an experiment in which all charged pions are detected, without energy discrimination. Cutting off the photon spectrum and integrating over photon energy gives the result that at electron energies well past resonance, say $Q=2.5$ μ, the inelastic corrections to pion pair production are as large as the cross section at that energy. However, as has been appropriately emphasized,[1] the inelastic radiative corrections are sensitive functions of experimental conditions and must be considered with a given experiment in mind.

For comparison, the cross sections for the similar process of $\mu^+ + \mu^-$ pair production are included here. The differential cross section in the barycentric frame of the electron-positron pair is[1,17,19]

[19] V. B. Berestetskii and I. Ia. Pomeranchuk, Soviet Phys.—JETP **29**, 580 (1956) (translation).

$$d\sigma/d\Omega=(\alpha^2/16)[(Q^2-\mu^2)^{\frac{1}{2}}/Q^3]\times[1+\cos^2\theta+(\mu^2/Q^2)\sin^2\theta], \quad (23)$$

and the total cross section is

$$\sigma=(\pi\alpha^2/3)[(Q^2-\mu^2)^{\frac{1}{2}}/Q^3][1+(\mu^2/2Q^2)], \quad (24)$$

where μ is the muon mass and Q is the electron or positron energy. The ratio of the pion pair production cross section (21) with $F(4Q^2)=1$ to the muon pair production cross section (24), is

$$\frac{\sigma_\pi}{\sigma_\mu}=\frac{1}{4}\frac{[1-(\mu_\pi^2/Q^2)]^{\frac{3}{2}}}{[1-(\mu_\mu^2/Q^2)]^{\frac{1}{2}}[1+(\mu_\mu^2/2Q^2)]}. \quad (25)$$

Since $\mu_\pi/\mu_\mu\approx\frac{4}{3}$, for energies well above threshold Eq. (25) can be expanded in μ^2/Q^2 to second order to give the more convenient approximation

$$\sigma_\pi/\sigma_\mu\approx\tfrac{1}{4}[1-\tfrac{3}{2}(\mu_\pi^2/Q^2)+\tfrac{1}{2}(\mu_\pi^4/Q^4)]. \quad (26)$$

Since Eq. (26) vanishes at the pion threshold, it becomes a satisfactory approximation to Eq. (25) even fairly near to threshold. For $Q=1.5\mu_\pi$, $\sigma_\pi/\sigma_\mu\approx0.1$, while in the extreme relativistic limit $\sigma_\pi/\sigma_\mu=\frac{1}{4}$. Comparing the differential cross sections Eqs. (20) and (23) indicates that (20) has a maximum for $\theta=90°$ while (23) has a minimum at the same value for θ. Thus the ratio of the pion differential cross section at $\theta=90°$ to the muon differential cross section at $\theta=90°$ is twice as large as the ratio of the total cross sections, Eqs. (25) and (26). However, $\pi-\pi$ interactions could alter the pion-to-muon ratio substantially.

ACKNOWLEDGMENTS

The author is indebted to Professor R. H. Dalitz for many helpful suggestions, and to Professor S. C. Wright for a helpful discussion.

APPENDIX

To illustrate the procedures of calculation, the calculations for reaction (4) are briefly described in this appendix. The Feynman diagrams are Figs. 1(b) and 1(c). Using Feynman's conventions,[3] the matrix element corresponding to Fig. 1(b) is

$$\mathfrak{M}_b=\frac{8\pi e^2 g}{\mu}\frac{\bar\psi(q_1')\gamma_\mu\psi(q_1)\bar\psi(-q_2)\gamma_\nu\psi(-q_2')\epsilon^{\alpha\mu\beta\nu}(q_1-q_1')_\alpha(q_2-q_2')_\beta}{(q_1-q_1')^2(q_2-q_2')^2}, \quad (A.1)$$

while the matrix element corresponding to Fig. 1(c) is

$$\mathfrak{M}_c=\frac{8\pi e^2 g}{\mu}\frac{\bar\psi(-q_2)\gamma_\mu\psi(q_1)\bar\psi(q_1')\gamma_\nu\psi(-q_2')\epsilon^{\alpha\mu\beta\nu}(q_1+q_2)_\alpha(q_1'+q_2')_\beta}{(q_1+q_2)^2(q_1'+q_2')^2}, \quad (A.2)$$

where $q_1(q_2)$ and $q_1'(q_2')$ are the initial and final four-momenta for the electron (positron). The matrix element for reaction (4) is the sum of (A.1) and (A.2).

In the usual way, the cross section is obtained by squaring the matrix element, averaging over the initial spin states, summing over the final spin states, and integrating over phase space ($\hbar=c=1$),

$$\sigma=\frac{1}{2}\int\frac{\langle|\mathfrak{M}|^2\rangle(2\pi)^7}{4Q_1Q_2}\delta(q_1+q_2-q_1'-q_2'-p)\delta(q_1'^2-m^2)\delta(q_2'^2-m^2)\delta(p^2-\mu^2)\frac{d^4q_1'd^4q_2'd^4p}{(2\pi)^{12}}. \quad (A.3)$$

The factor $\frac{1}{2}$ is the flux factor appropriate for these relativistic energies. The approximation $m^2=0$ is used except when it would result in a divergent cross section. In this last case the lowest-order term in m^2 is also kept.

It is most convenient to do the integrations over the electron-positron phase space in their barycentric frame in terms of the variables $r=q_1'+q_2'$ and $s=q_1'-q_2'$. The phase space expression in (A.3) is modified by the relation

$$\delta(q_1'^2-m^2)\delta(q_2'^2-m^2)=\tfrac{1}{4}\delta(r\cdot s)\delta(r^2+s^2-4m^2). \quad (A.4)$$

The momentum-energy conservation delta function is eliminated in the integration over r. The delta functions (A.4) are eliminated by two of the integrals over s, leaving the angular integrations of s. Two important integrals over angle that occur are of the form

$$\int\frac{d\Omega_s}{(1-\beta_1\hat s\cdot\hat q_1)(1+\beta_2\hat s\cdot\hat q_2)}=\frac{2\pi}{K^{\frac{1}{2}}}\ln\frac{1+\beta_1\beta_2\hat q_1\cdot\hat q_2+K^{\frac{1}{2}}}{1+\beta_1\beta_2\hat q_1\cdot\hat q_2-K^{\frac{1}{2}}}, \quad (A.5)$$

and

$$\int\frac{(\hat q_1\times\hat q_2\cdot\hat s)^2d\Omega_s}{(1-\beta_1\hat s\cdot\hat q_1)^2(1+\beta_2\hat s\cdot\hat q_2)^2}=\frac{4\pi}{K}(\hat q_1\times\hat q_2)^2-\frac{2\pi}{K^{\frac{3}{2}}}(\hat q_1\times\hat q_2)^2(1+\beta_1\beta_2\hat q_1\cdot\hat q_2)\ln\frac{1+\beta_1\beta_2\hat q_1\cdot\hat q_2+K^{\frac{1}{2}}}{1+\beta_1\beta_2\hat q_1\cdot\hat q_2-K^{\frac{1}{2}}}, \quad (A.6)$$

where

$$K=(1+\beta_1\beta_2\hat q_1\cdot\hat q_2)^2-(1-\beta_1^2)(1-\beta_2^2).$$

After the integrations have been performed, one must perform a Lorentz transformation parallel to the momentum of the pion, **P**, in order to return to the barycentric frame of the initial electron-positron system. The parameter for this Lorentz transformation is

$$\beta = P/(2Q-E). \tag{A.7}$$

Eliminating the remaining delta function by integrating over the meson energy variable E results in the spectral-differential cross section, Eq. (17).

It was found that not all of the integrations over meson angles in Eq. (17) were possible in terms of tabulated functions. However, when the terms were collected according to whether they would contribute as $[\ln(2Q/m)]^2$, $\ln(2Q/m)$, or unity, to the total cross section, it was possible to do the integrations over meson angles for the terms proportional to $[\ln(2Q/m)]^2$ and $\ln(2Q/m)$. Since $\ln(2Q/m)\approx 6$, these two sets of terms are also the most important. In order to verify this, the nonlogarithmic contributions to the pion spectrum were evaluated numerically for $Q=1.0\mu$ and $P=0.1\mu$, 0.4μ, and 0.74μ. The values obtained for the nonlogarithmic corrections relative to the logarithmic contributions were $+0.2\%$, -1.3%, and $+5.4\%$, respectively.

PHYSICAL REVIEW VOLUME 123, NUMBER 2 JULY 15, 1961

Optimal Measuring Apparatus

MUTSUO M. YANASE*
Palmer Physical Laboratory, Princeton University, Princeton, New Jersey
(Received March 6, 1961)

An upper limit for the accuracy of the measurement of a simple quantity which does not commute with a conserved quantity is obtained in terms of the "size" of the apparatus. The "size" of the apparatus is defined as the mean square value $\hbar^2M^2$ of the conserved quantity for the apparatus which is, in the example chosen, the z component of the angular momentum. The measured quantity is the projection of a spin in a perpendicular direction. It is found that the probability of an unsuccessful measurement is at least $1/8M^2$.

1. INTRODUCTION

IT was shown recently that a quantum mechanical operator which does not commute with the operator of a conserved quantity can be measured only approximately. There is a finite probability that the measurement is unsuccessful, but this probability can be very small if the measuring apparatus contains a large amount of the conserved quantity.[1] It was shown, in particular, that if the product of the probability of an unsuccessful measurement and of the maximum value of the conserved quantity which is present in the measuring apparatus exceeds a certain value, no contradiction with the conservation law occurs. The objective of the present article is to find the "best" measuring apparatus for a given "size." The conserved quantity will not have an upper limit in the initial state of this; rather, we specify the mean-square value of the conserved quantity and ask for the minimum probability for an unsuccessful measurement, consistent with the prescribed mean square of the conserved quantity and, of course, the validity of the conservation law.

We require that the operator of the conserved quantity for the apparatus commute with the operator, by which the final state of the apparatus is measured. This condition is necessary because otherwise—as a consequence of the result of our previous work—we cannot ascertain the result of the measurement exactly.

The condition to be obtained will be only a necessary one. In other words, for the given mean square of the conserved quantity, the probability of a malfunctioning of the apparatus cannot be smaller than the value to be calculated. Whether an apparatus with the specified properties is actually possible will not be decided. All that can be claimed is that the existence of such an apparatus is not in conflict with the conservation law considered.

The quantity to be measured and the conservation law to be considered will be the same as in the first publication on this subject: The quantity is the component of the spin of a particle in a given direction; the conserved quantity, the angular momentum about a direction perpendicular to the aforementioned direction. It will be shown in Sec. 2 that the minimum probability for the malfunctioning of the apparatus is inversely proportional to the mean square of the conserved quantity, and the proportionality constant will be determined. Section 3 will contain a discussion of the results.

2. MINIMIZATION OF THE MALFUNCTIONING PROBABILITY

We measure the x component of the spin of a particle with spin $\frac{1}{2}$; the z component of the spin of this particle is the additive conserved quantity. To make the compu-

* On leave of absence from Sophia University, Tokyo, Japan.
[1] E. P. Wigner, Z. Physik **131**, 101 (1952); H. Araki and M. M. Yanase, Phys. Rev. **120**, 622 (1960).